Regularized Geometric Hulls for Nucleus Segmentation in Microscopy Images

Marco Körner
marco.koerner@uni-jena.de
Mahesh V. Krishna
mahesh.v.krishna@uni-jena.de
Herbert Süße
herbert.suesse@uni-jena.de
Wolfgang Ortmann
wolfgang.ortmann@uni-jena.de
Joachim Denzler
joachim.denzler@uni-jena.de

Computer Vision Group
Friedrich Schiller University of Jena
Jena, Germany
http://www.inf-cv.uni-jena.de

Abstract

As segmentation of cells from microscopy images is a very complex and error-prone task, we present a new unsupervised and fully-automatic method based on *Regularized Geometric Hulls (RGH)*. While it performs up to two orders of magnitudes faster than state-of-the-art methods, wide-range experiments performed on the recent *CellCognition* dataset demonstrate its robustness and accuracy.

1 Introduction

During the decades of research in the field of microscopy-based tissue analysis, the identification and segmentation of individual cells is one of, if not the most important and fundamental step within the whole processing pipeline. While classically this task had to be performed manually, more and more automatic or semi-automatic methods came into the focus of modern computer vision research. As this problem is highly affected by image degradations such as blur or pixel noise, traditional contour segmentation methods are likely to fail in these scenario. Furthermore, other approaches require manual annotation of cells for localization or employ computationally expensive machine learning techniques for building complex models of cell appearance. Segmentation of cells from images has been tackled with a wide variety of tools, ranging from simple thresholding to machine learning-based methods [5]. Many of them tackle specific types of microscopy images and are application specific.

For instance, approaches based on *Seeded Watershed Transform* are well-established for cell segmentation [6]. However, the quality of the results depend heavily on the initial seeds and the approach often produces over-segmented images. These shortcomings necessitate further processing steps, which result in computationally complex algorithms, and a different approach is called for. Other popular approaches use machine learning methods. Arteta *et al.* [1] employ a SVM classifier for categorizing each pixel to belong to either cell foreground or

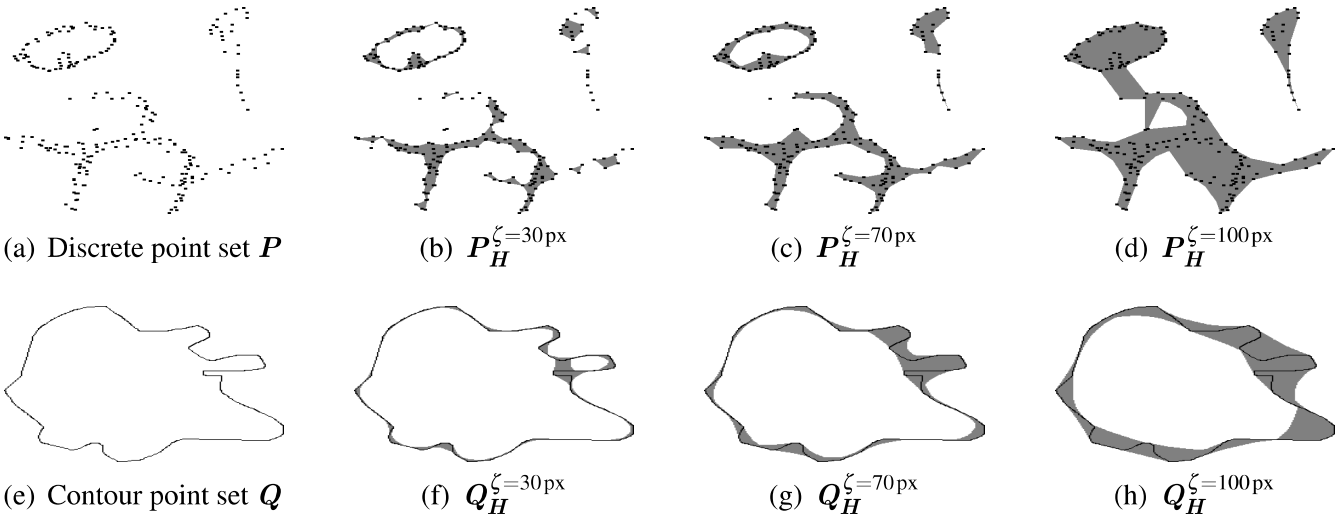

(a) Discrete point set $\boldsymbol{P}$ (b) $\boldsymbol{P}_H^{\zeta=30\text{px}}$ (c) $\boldsymbol{P}_H^{\zeta=70\text{px}}$ (d) $\boldsymbol{P}_H^{\zeta=100\text{px}}$

(e) Contour point set $\boldsymbol{Q}$ (f) $\boldsymbol{Q}_H^{\zeta=30\text{px}}$ (g) $\boldsymbol{Q}_H^{\zeta=70\text{px}}$ (h) $\boldsymbol{Q}_H^{\zeta=100\text{px}}$

Figure 1: Influence of different values for the regularization parameter ζ on geometric hull construction for the case of (a)–(d) dense point sets and (e)–(h) contour point sets. Note that the RGH preserves inner contours.

background. This binarization is further analyzed for connected components to achieve final segmentation results. While this approach shows promising results, pixel-wise operations on high-dimensional image sequences common in time-lapse microscopy videos make it unsuitable for fast processing. Furthermore, it depends on the availability of manually labeled training data, which is often difficult or impossible to supply.

In contrast, we propose a method for fast and robust joint cell detection and segmentation based on *Regularized Geometric Hulls (RGH)* [7] which is designed to be unsupervised, acting fully automatic, and requires only one rather simple parameter to be adjusted.

2 Regularized Geometric Hull

This section is dedicated to briefly introduce into the concept of *Regularized Geometric Hulls (RGH)* recently presented by Süße *et al.* [7], which is the core ingredient of our proposed method. These can be regarded as an extension of classical convex hulls.

Definition 1 (Convex hull)**.**
Given an arbitrary set of Euclidean points $\boldsymbol{P} = \left\{\boldsymbol{p} | \boldsymbol{p} \in \mathbb{R}^2\right\}$ *(or discrete lattice points* $\boldsymbol{Q} = \left\{\boldsymbol{q} | \boldsymbol{q} \in \mathbb{Z}^2\right\}$*), the* Convex Hull $\boldsymbol{P}_H \supseteq \boldsymbol{P}$ *(*$\boldsymbol{Q}_H \supseteq \boldsymbol{Q}$*) is the smallest convex subset of* $\mathbb{R}^2$ *that contains* $\boldsymbol{P}$ *(*$\boldsymbol{Q}$*).*

Various algorithms for the computation of the convex hull with fair runtime complexity $\mathcal{O}(n \log n)$ exist in the field of computational geometry. As this convex hull approximation of points is insufficiently coarse for most computer vision problems, we aim to allow a certain degree of non-convexity—*i.e.* concavity—while computing geometric hulls.

Definition 2 (adjacent points)**.**
Let $d : \boldsymbol{M}^2 \mapsto \mathbb{R}$ *be a metric in* $\boldsymbol{M}^2$*. Two points* $\boldsymbol{p}, \boldsymbol{q} \in \boldsymbol{M}^2$ *are called* ζ-adjacent *wrt. a non-negative constant* $0 \leq \zeta \in \mathbb{R}$*, if*

$$\boldsymbol{p} \sim^{\zeta} \boldsymbol{q} \Leftrightarrow d(\boldsymbol{p}, \boldsymbol{q}) \leq \zeta \quad . \tag{1}$$

Definition 3 (Regularized Geometric Hull (RGH) for Euclidean point sets)**.**
Let $\boldsymbol{P} = \left\{\boldsymbol{p} | \boldsymbol{p} \in \mathbb{R}^2\right\}$ *be an arbitrary set of Euclidean points and* $\Delta(\boldsymbol{p}_1, \boldsymbol{p}_2, \boldsymbol{p}_3) \subseteq \boldsymbol{P}$ *the set of all points* $\boldsymbol{p}_i \in \boldsymbol{P}$ *enclosed by the triangle defined by the 3-tuple* $(\boldsymbol{p}_1, \boldsymbol{p}_2, \boldsymbol{p}_3) \in \boldsymbol{P}^3$*.*

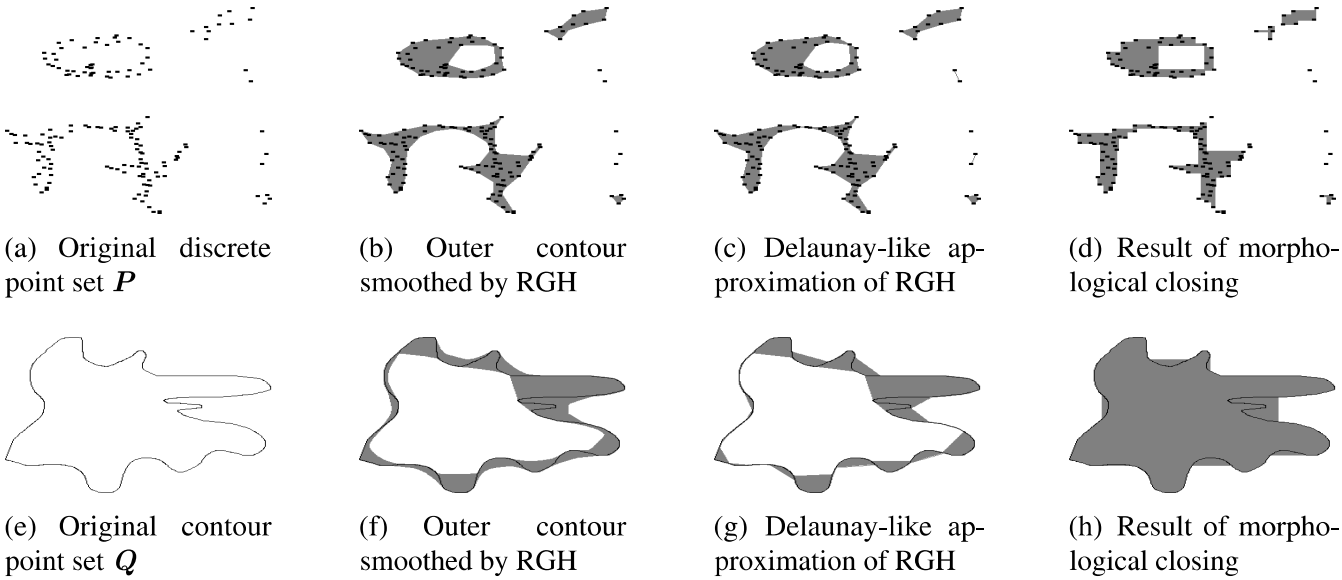

(a) Original discrete point set $\boldsymbol{P}$ (b) Outer contour smoothed by RGH (c) Delaunay-like approximation of RGH (d) Result of morphological closing

(e) Original contour point set $\boldsymbol{Q}$ (f) Outer contour smoothed by RGH (g) Delaunay-like approximation of RGH (h) Result of morphological closing

Figure 2: The *RGH* can be approximated by using Delaunay-like triangulations of the input point cloud $\boldsymbol{P}$ or contour $\boldsymbol{Q}$, which realizes a morphological closing operation with adaptive, polygonial structure elements.

Further, let

$$\boldsymbol{P}_{\Delta}^{\zeta} = \left\{ \Delta(\boldsymbol{p}_1, \boldsymbol{p}_2, \boldsymbol{p}_3) \in \boldsymbol{P}^3 \mid \boldsymbol{p}_1 \sim^{\zeta} \boldsymbol{p}_2 \wedge \boldsymbol{p}_2 \sim^{\zeta} \boldsymbol{p}_3 \wedge \boldsymbol{p}_1 \sim^{\zeta} \boldsymbol{p}_3 \right\}, \quad 0 \leq \zeta \in \mathbb{R}, \tag{2}$$

be the set of all triangles of ζ-adjacent points in $\boldsymbol{P}$. Then, the union set

$$\boldsymbol{P}_{H}^{\zeta} = \bigcup \boldsymbol{P}_{\Delta}^{\zeta} \cup \boldsymbol{P} \tag{3}$$

is called the Regularized Geometric Hull (RGH) *of $\boldsymbol{P}$ wrt. ζ.*

Definition 4 (Regularized Geometric Hull (RGH) for discrete lattice point sets)**.**
Let $\boldsymbol{Q} = \left\{ \boldsymbol{q} | \boldsymbol{q} \in \mathbb{Z}^2 \right\}$ be an arbitrary set of discrete lattice points and $\Delta(q_1, q_2, q_3) \subseteq \boldsymbol{Q}$ the set of all triangular points $\boldsymbol{q}_i \in \boldsymbol{Q}$ induced by the lattice points $(\boldsymbol{q}_1, \boldsymbol{q}_2, \boldsymbol{q}_3) \in \boldsymbol{Q}^3$. Let further be

$$\boldsymbol{Q}_{\Delta}^{\zeta} = \left\{ \Delta(\boldsymbol{q}_1, \boldsymbol{q}_2, \boldsymbol{q}_3) \in \boldsymbol{Q}^3 \mid \boldsymbol{q}_1 \sim^{\zeta} \boldsymbol{q}_2 \wedge \boldsymbol{q}_2 \sim^{\zeta} \boldsymbol{q}_3 \wedge \boldsymbol{q}_1 \sim^{\zeta} \boldsymbol{q}_3 \right\}, \quad 0 \leq \zeta \in \mathbb{R}, \tag{4}$$

the set of all non-degenerated *triangles of ζ-adjacent points in $\boldsymbol{Q}$. Then, the union set*

$$\boldsymbol{Q}_{H}^{\zeta} = \bigcup \boldsymbol{Q}_{\Delta}^{\zeta} \cup \boldsymbol{Q} \tag{5}$$

is called the Regularized Geometric Hull (RGH) *of $\boldsymbol{Q}$ wrt. ζ.*

Clearly, the properties of the geometric hull $\boldsymbol{P}_{H}^{\zeta}$ strictly depend on the choice of the structure parameter ζ, as can be seen in Fig. 1. If $\zeta = 0$, the geometric hull $\boldsymbol{P}_{H}^{0}$ is identical to the point set $\boldsymbol{P}$. In turn, if $\zeta \to \infty$, the geometric hull $\boldsymbol{P}_{H}^{\zeta}$ converges to the convex hull $\boldsymbol{P}_{H}$ yielding the relation

$$\boldsymbol{P} = \boldsymbol{P}_{H}^{0} \subseteq \boldsymbol{P}_{H}^{\zeta} \subseteq \boldsymbol{P}_{H}^{\infty} = \boldsymbol{P}_{H}, \quad 0 \leq \zeta \in \mathbb{R}. \tag{6}$$

The structure parameter ζ regularizes the convexity or concavity of the geometric hull. In contrast to the classical convex hull $\boldsymbol{P}_{H}$, the RGH $\boldsymbol{P}_{H}^{\zeta}$ describes the geometric structure of the input data $\boldsymbol{P}$ by a set of outer and inner contours.

2.1 Approximation

Def. 3 and 4 suggest that the computation of the RGH shows cubic complexity $\mathcal{O}(n^3)$ in the number n of input points which makes its application unhandy in realistic scenarios. For this

reason, we approximate the underlying set of triangles $\boldsymbol{P}_\Delta^\zeta \subseteq \boldsymbol{P}^3$ by a modification of the *Delaunay triangulation* [2] $\boldsymbol{P}_\Delta^{\zeta_{\mathrm{DT}}} \subseteq \boldsymbol{P}^3$, which is supposed to be a triangular tessellation of a given point set $\boldsymbol{P}$ optimal wrt. a given distance criterion. All triangles obtained by Delaunay's triangulation algorithm are drawn into a binary image, wherefrom final contours are extracted afterwards. Hence, the Delaunay triangulation $\boldsymbol{P}_\Delta^{\zeta_{\mathrm{DT}}}$—restricted to triangles with edge lengths smaller than $0 \leq \zeta \in \mathbb{R}$—can be interpreted as an approximation of the previously used set $\boldsymbol{P}_\Delta^\zeta$ of triangles of ζ-adjacent points. The images shown in Fig. 2(c) and 2(g) show the results of the RGH algorithm using the Delaunay-like approximation for both a discrete point set and a set of discrete contour points, respectively. Compared to the results of the original RGH algorithm shown in Fig. 2(b) and 2(f), the results are reasonably good and useful for further processing. As the Delaunay algorithm shows solely quasi-logarithmic complexity $\mathcal{O}(n \log n)$ in the number n of vertices, this approximation remarkably speeds up the whole computation and allows for real-time performance.

2.2 Geometric Interpretation

When analyzing the results of the RGH or their approximation based on Delaunay triangulation, one can observe various handy properties useful for further processing of precomputed contours or point sets. First, the RGH augments the input contour or dense point set $\boldsymbol{P}$ by a *geometric orientation*, enabling us to easily apply neighborhood-based methods for shape recognition. While doing so, in the case of discrete point sets and dependent from the structure parameter ζ, existing holes are preserved and isolated objects are detected, as can be seen in Fig. 2(b) and (c).

Second and as illustrated in Fig. 2, the presented method performs a *smoothing* of a given contour which can be used to deal with inaccurate segmentation. Again, the impact of this smoothing is tuned by the structure parameter ζ. In terms of computational geometry, this is comparable to the *morphological closing* operator applied to binary objects. So, RGHs can be characterized as such a closing operation based on adaptive, polygonial structure elements. In contrast to classical morphological closing with constant regular structure elements (*e.g.* rectangles, ellipses), the results of RGHs constructed from contours or dense point sets appear much more smooth and intuitive, as can be seen in Fig. Fig. 2(d) and (h), respectively.

3 Evaluation

3.1 Dataset

As annotated image data of cells is very rare, most of the existing approaches were evaluated on rather small non-public databases. For instance, Arteta *et al.* [1] used three datasets of 12 to 22 images in their experiments. In contrast, the *CellCognition* dataset presented by Held *et al.* [4] consists of 7 sequences of 206 frames of size 1392×1040 px, each showing RNAi treated human HeLa Kyoto cells expressing fluorescent H2B-mCherry (orange) and α-tubulin (green). In total, the dataset contains 363,120 annotated cell objects with automatically generated ground truth data providing centroids and bounding boxes. Fig. 3 shows an example frame of the data-set, with the full recording and the segregated nuclei. Apart from the huge number of objects, the data-set is made more challenging by low contrast in many cases, and overlapping cells due to limits in the thinness of slide preparations.

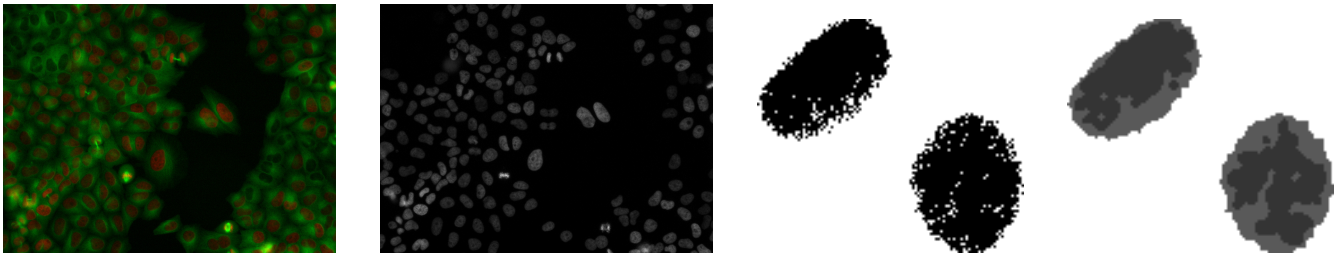

(a) microscopic image (b) corresponding nuclei expressing H2B-mCherry (c) Thresholded nuclei (d) RGH result

Figure 3: Images from the CellCognition dataset (a) are initially thresholded (c) and further used to extract nuclear boundaries by RGH (d).

3.2 Experimental Setup

As the proposed method is designed in a very general way, the overall framework is rather straightforward. After binary thresholding the input images (*cf*. Fig. 3(c)), they are directly passed to the RGH module to create foreground-background images as exemplary shown in Fig. 3(d). The values of the structure parameter ζ are varied in order to show its influence on the overall results. Cells are finally extracted by subsequent contour extraction.

For comparison to other methods we used two popular quantification methods. First, suggested by Arteta *et al*. [1], we assumed each cell detected by our system to be a true positive, if the distance between its centroid and the centroid of the nearest ground truth cell is smaller than a predefined threshold ρ_{dist}. Usually, this threeshold is set to the radius of the smallest cell expected to appear in the data. Second and more commonly used in object detection, a detected cell is assumed to match a ground truth cell if the ratio

$$r\left(B_{\text{det}}, B_{\text{gt}}\right) = \frac{\text{area}\left(B_{\text{det}} \cap B_{\text{gt}}\right)}{\text{area}\left(B_{\text{det}} \cup B_{\text{gt}}\right)} \tag{7}$$

of the union and intersection areas of respective bounding boxes B_{det} and B_{gt} exceeds the value of $\rho_{\text{area}} = 0.5$ (*cf*. *Pascal Criterion* [3]).

3.3 Results

In order to evaluate the performance of our methods, we compared to the state-of-the-art method presented by Arteta *et al*. [1]. From the numbers reported in Tab. 1, it can be observed that our approach performs better or at least comparable to the competing method. Intuitively, the structure parameter ζ only slightly influences the overall accuracy. Wrong segmentation mainly occurs when two objects are closer than the structure parameter ζ. Furthermore it has to be noted that the evaluation based on cell centroid distances yields higher accuracy. This should be taken into account for further comparisons. The most remarkable observation arises from the computational analysis. While the supervised method of Arteta *et al*. [1] requires a very time-consuming training phase, even the testing step is rather slow. In contrast, our approach performs localization and segmentation almost two orders of magnitudes faster, which is a great advantage in real-world applications.

4 Summary

We proposed a method for detecting and segmenting cell in microscopy images relying on *Regularized Geometric Hulls (RGH)* only incorporating one single parameter which is easy to

Method	Accuracy		Runtime	
	Centroid distance $\rho_{\text{dist}} = 20\,\text{px}$	Pascal criterion $\rho_{\text{area}} = 0.5$	training	testing
our approach			—	1.96 s/frame
$\zeta = 3\,\text{px}$	91.65%	85.75%		
$\zeta = 4\,\text{px}$	91.75%	85.01%		
$\zeta = 5\,\text{px}$	92.11%	85.77%		
Arteta *et al.* [1]	88.79%	86.20%	6231.59 s	130.66 s/frame

Table 1: Evaluation of our approach and comparison to state-of-the-art methods.

tune. In contrast to competing approaches, our method does not require any supervision, prior learning phases or manual annotation. Extensive experiments on the recent *CellCognition* dataset verified the accuracy of our approach and demonstrated its superior runtime behavior.

Subjected to future work, we intend to predict the structure parameter ζ adaptively while segmentation or learn it from training data and to use more sophisticated preprocessing of the input data compared to binary thresholding as used in our framework.

Acknowledgements

The authors thank Christian Wojek and Stefan Saur for useful discussions and suggestions. Mahesh Venkata Krishna is supported by Carl Zeiss AG through the “Pro-Excellenz” scholarship of the Federal State of Thuringia, Germany.

References

[1] C. Arteta, V. Lempitsky, J. Noble, and A. Zisserman. Learning to detect cells using non-overlapping extremal regions. In *MICCAI*, pages 348–356. Springer-Verlag, 2012.

[2] B. Delaunay. Sur la sphère vide. *USSR Academy of Sciences*, (6):793–800, 1934.

[3] M. Everingham, L van Gool, C. Williams, J. Winn, and A. Zisserman. The pascal visual object classes (voc) challenge. *IJCV*, 88(2):303–338, 2010.

[4] M. Held, M. Schmitz, B. Fischer, T. Walter, B. Neumann, M. Olma, M. Peter, J. Ellenberg, and D. Gerlich. Cellcognition: Time-resolved phenotype annotation in high-throughput live cell imaging. *Nature Methods*, 7(9):747–754, 2010.

[5] E. Meijering. Cell segmentation: 50 years down the road. *Signal Processing Magazine, IEEE*, 29(5):140–145, Sept 2012.

[6] F. Meyer and S. Beucher. Morphological segmentation. *Journal of Visual Communication and Image Representation*, 1(1):21–46, 1990.

[7] H. Süße, W. Ortmann, J. Lautenschläger, C. Lautenschläger, M. Körner, J. Großkreutz, and J. Denzler. Quantitative analysis of pathological mitochondrial morphology in neuronal cells in confocal laser scanning microscopy images. In *IWBBIO*, pages 1290–1301, 2014.